ASTARTE

Assessment, STrategy And Risk Reduction for Tsunamis in Europe

Grant Agreement no: 603839
Organisation name of lead contractor: IPMA
Coordinator: Maria Ana Baptista

Deliverable 5.30
Performance of different types of breakwaters and coastal protection structures under tsunami attack

Due date of deliverable:	M36
Actual submission date:	M41
Start date of the project:	11/2013
Duration:	42 months

Work Package:	5 "Tsunami-coastal impacts"
Lead beneficiary of this deliverable:	UC
Author(s):	**UC**: Íñigo Aniel-Quiroga, César Vidal, Mauricio González, Javier López Lara, Ahmet Yalciner, Gokhan Guler, David Fuhrman

Project co-funded by the European Commission within the Seventh Framework Programme (2007-2013)	
Dissemination Level	
PU Public	X
PP Restricted to other programme participants (including the Commission Services)	
RE Restricted to a group specified by the consortium (including the Commission Services)	

CO Confidential, only for members of the consortium (including the Commission Services)	

TABLE OF CONTENTS

EXECUTIVE SUMMARY

ASTARTE (Assessment STrategy And Risk for Tsunami in Europe) project aims to develop a comprehensive strategy to mitigate tsunami impact in The NEAM (North East Atlantic, Mediterranean and Adjacent Seas) region of IOC/UNESCO. Within the project, Work Package 5 focuses on gaining a better understanding of tsunami impacts in coastal areas and on structures. The WP5 aim is to study the stability and performance of coastal defenses, critical and strategic structures, to identify lessons and new innovative and cost-effective design concepts and solutions for coastal and marine structures, and to investigate the tsunami-induced boundary layer, sediment transport, and morphological changes on coastal areas.

In order to improve the current knowledge and experience on the interaction between marine structures and tsunamis, physical experiments on rubble-mound breakwaters (RMB) under tsunami attack have been carried out. These experiments help in the addition of the tsunami dimension to the design process of structures that are located in the tsunami affection areas. The Deliverable 5.30 presents the assessment of the stability of rubble mound breakwaters based on the laboratory experiments focus on the calculation of the damage that each experiment prompts on the structures. This analysis presents the performance of rubble mound breakwaters in case of tsunami, and the results can be applied in D 9.47 to develop guidelines to design more resilient structures that help to mitigate tsunami risk.

DOCUMENT INFORMATION

Project Number	FP7 - 603839	**Acronym**	ASTARTE
Full Title	Assessment, STrategy And Risk Reduction for Tsunamis in Europe		
Project URL	http://www.astarte-project.eu/		
Document URL			
EU Project Officer	Denis Peter		

Deliverable	**Number**	D5.30	**Title**	Performance of different types of breakwaters and coastal protection structures under tsunami attack
Work Package	**Number**	WP5	**Title**	Tsunami-coastal impacts

Date of Delivery	**Contractual**	M36	**Actual**	M41
Status	version 0.1		final □	
Nature	prototype □ report ☑ dissemination □			
Dissemination level	public ☑ consortium □			

Authors (Partner)	Íñigo Aniel-Quiroga (UC), Mauricio González (UC)			
Responsible Author	**Name**	Íñigo Aniel-Quiroga	**E-mail**	anieli@unican,es
	Partner	UC	**Phone**	+34 942201616

LIST OF FIGURES

1. INTRODUCTION

The WP5 of ASTARTE project focuses on gaining a better understanding of tsunami impacts on coastal areas. One of the main objectives of the WP5 is the study of stability and performance of coastal structures. Therefore, as part of this WP5, in the framework of the Task 5.1 laboratory experiments on marine structures under tsunami waves have been conducted at the IH Cantabria facilities in Santander, Spain. These physical experiments aim on advancing in the knowledge on how these structures respond under tsunami attack. Improving the knowledge about their stability conditions and hydrodynamics will enhance the design of coastal protection marine structures, and will contribute to mitigate the consequences of these extreme events.

It is necessary that dikes and breakwaters maintain some functionality in case of tsunami, in order to contribute to the mitigation of the tsunami effects. Among coastal structures, the response of vertical concrete structures against tsunamis has been already addressed by several authors, e.g. Asakura et al., (2002) [3], Kato et al., (2006) [4], Mizutani et al., (2001) [5], or Nistor et al (2009) [6]. However, the effectiveness and stability of rubble mound breakwaters (RMB) against tsunamis has not been sufficiently studied. RMB are usually designed to support adequately the loads generated by wind waves but tsunami actions are not taken into account in the design. In view of this, laboratory experiments on 2 typologies of rubble-mound breakwaters were addressed: with and without crown-wall.

The characteristics of these laboratory experiments were profusely explained in the Deliverable D5.21 of ASTARTE project. The data measured on part of these tests were transferred as well to WP4. In the framework of the D4.20, they were included to be used as benchmark to calibrate and validate numerical models that perform the propagation, inundation and interaction of tsunamis with coastal structures.

Complementing the commented deliverables, D5.30 aims to evaluate the performance of the RMBs in the experiments. The damage triggered by each tsunami-like wave was measured what allowed to tackle the study of stability by means of classical analysis of damage parameters. As a consequence, these analyses allow to explain the differences on their behavior when they work under wind waves or under tsunami waves, what will help in the proposal of new methods or formulas that improve their design and performance in case of tsunami (Deliverable 9.47)

The document of the D5.30 is organized as follows:

- In the chapter 2, an introduction to the topic of the differences between the performance of the structures under wind waves and tsunami waves is addressed, focused on showing the real problem that these structures face.
- In the chapter 3, a brief summary of the characteristics of the modeled structures is given.
- In the chapter 4, an analysis of the currently existing way to simulate tsunamis in the lab is carried out, and these lab experiments methodology is briefly explained.

- In the chapter 5, the variables that have been included in the analyses are introduced and explained
- Finally, in the chapter 6, the results of the experiments, and the performance of the RMBs are addressed.

2. PERFORMANCE OF COMMON RMB UNDER TSUNAMI WAVE: FORMULATION OF THE PROBLEM

The design and performance of RMB under wind waves have been profusely addressed in the past. The design normally includes the loads that regular and extreme swell can generate in the different parts of the structure. However, as commented in the introduction, tsunami loads are not taken into account due to their low recurrence. Furthermore, when the incorporation of tsunami actions is addressed it is required to determine if the methodologies and results that are normally applied and obtained for ordinary wind waves, are directly applicable or not. In other words, it is required to study if a similarity hypothesis can be assumed or if it is necessary to adapt or particularize these techniques and methodologies to the case of tsunamis.

When a set of wind waves reaches the outer slope of a RMB, the waves transform and break, run up, eventually overtop the crown-wall, and finally they are reflected to the sea and transmitted through the core. Any flow variable on the slope, like run-up and run-down, velocities, etc., depend on the incident waves characteristics, the geometry of the structure, the nearby bottom and the water itself (wave height, period and direction, bottom and structure slopes, type of armour units, filter layer and core, water density and viscosity, etc.). The analytic determination of the stability of the breakwater has some limitations (e.g. calculation and validation of flux coefficients) and, consequently, it is commonly tackled by measuring the damage on laboratory experiments that are used to fit empirical damage formulae. Besides, a part of the wave is transmitted to the protected area in two ways: by overtopping the structure crown, when wave heights are enough to achieve it and by passing through the layers of the RMB, including the core. The interaction between the waves and the structure is punctual, short and fast. The main damaged area is usually the seaside slope, where the action of the gravity and the run-down of the waves is combined to displace the armour units. The damage on the leeside slope is prompted by the eventual overtopping of high enough waves.

However, the action of a tsunami is different and the response of the structure, too. Most of the existing rubble mound breakwaters are finite length structures protecting harbors or the coast. When a tsunami wave enters the continental shelf, the leading part of the tsunami wave may split in bore-like solitons, while the sea level rises and ebbs during the long-period waves. When the solitons or bores hits a breakwater, heavy run-up and overtopping occurs, producing damage in the outer slope, the crest and specially in the inner slope that is not usually designed for such heavy overflows. In addition, the transmission rate is higher and the shoreward interstitial flow pushes the back slope stones out of the armor. If the breakwater has a wave screen (crown-wall), the high horizontal and

vertical pressures induced by the flow may also induce the sliding or overturning of the structure. The overflow created by the slower increase of the sea level of the tsunami wave also tends to damage the rear slope, but as the tsunami wave also propagates through the breakwater head (and over it) the sea level increases in the leeside and the flow action on the rear slope decreases.

3. LABORATORY EXPERIMENTS SUMMARY

The physical experiments carried out in the laboratory are based on real marine structures. The breakwater models that have been tested are scaled versions of typical Mediterranean rubble mound breakwaters built to protect small fishing ports and marinas. These structures are not designed to deal with tsunami actions and, therefore, it is crucial to study their behavior in case of tsunami as a first step to improve their performance to contribute to reduce the tsunami consequences. Two typologies of rubble-mound breakwaters have been chosen: with crown wall (Type I) and without crown wall (Type II).

In Figures 1 and 2 transversal sections of type I and type II rubble-mound breakwaters, respectively, can be observed, including the installed instrumentation.

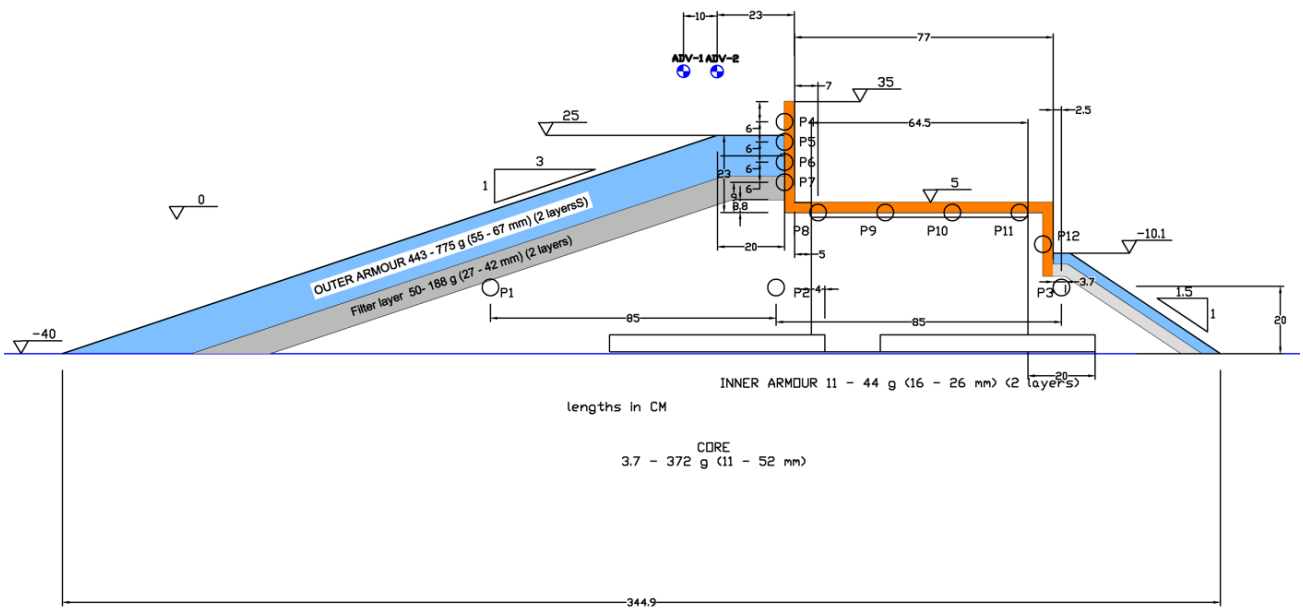

Figure 1. Rubble-mound breakwater with crown-wall (type I) transversal section

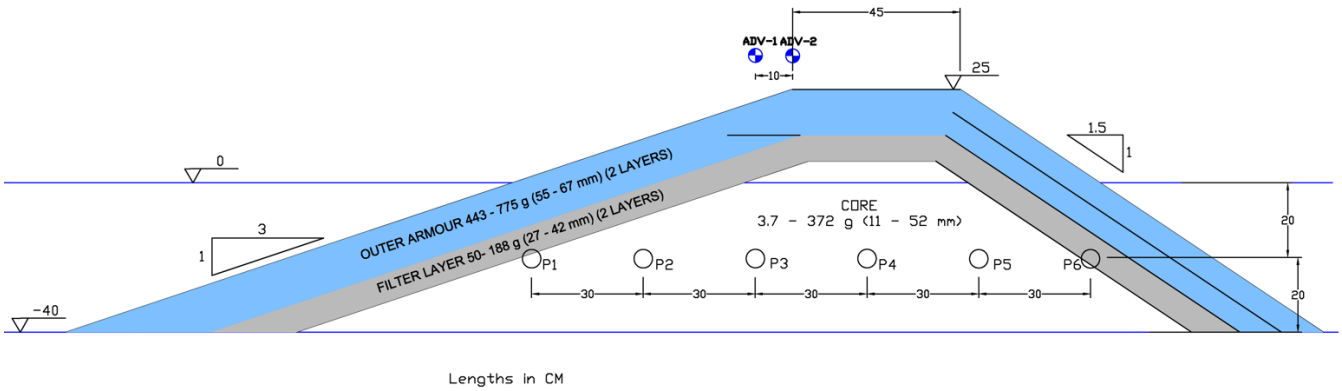

Figure 2. Rubble-mound breakwater without crown-wall (type II) transversal section

The experiments were conducted in the facilities of the University of Cantabria in Santander. The flume dimensions are: length, 56 m; maximum depth, 2.5 m; and width, 2 m (Figure 3). The flume has a 24 m long test section with sides and bottom made of transparent glass. The structures to be tested are located in this section. It also includes a shoaling ramp (4.71H/0.35V) before the test section.

Figure 3. Tsunami-wave flume at IH Cantabria facilities in Santander. The test section in the middle of the flume has sides and bottom made of transparent glass.

In Figure 4 a simplified scheme of the geometry of the flume is shown.

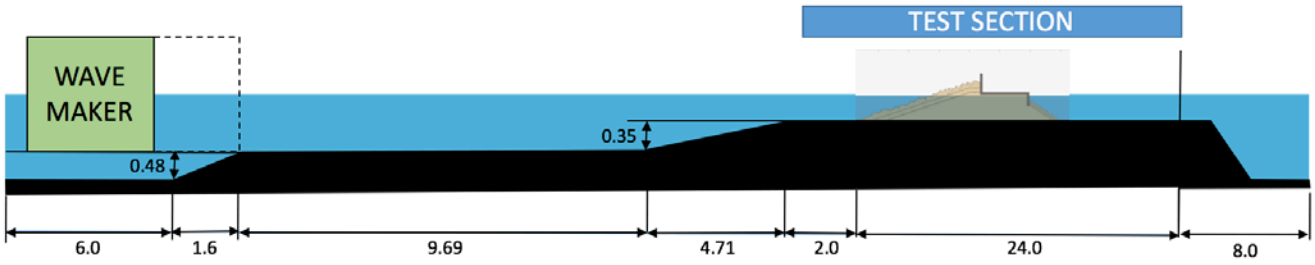

Figure 4. Simplified scheme of the geometry of the IH Cantabria tsunami flume

The following devices were installed in the flume and in the breakwaters to measure free surface displacement, hydrodynamic loads, and current velocity:

- A total of 9 wave gauges (WG) were installed along the flume. Six WGs where installed in the seaside and the other 3 in the harbor side (Fig. 5).

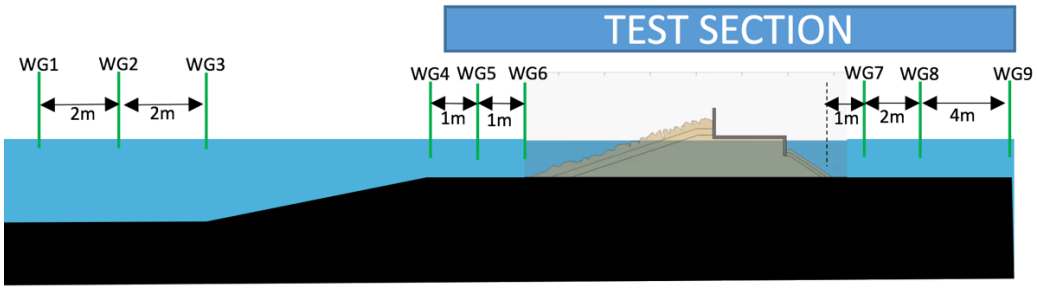

Figure 5. Scheme of the position of the wave gauges (WG) in the flume

- Several pressure gauges were installed inside both structures. For type I model (with crown wall), a total of 12 pressure sensors were used, 3 of them inside the core, near the filters layers and also in the middle, see Figure 1. The other 9 pressure sensors were placed in the crown-wall. For type II model (without crown-wall), a total of 6 pressure sensors were installed, all of them inside the core of the structure, see Figure 2.
- Water velocity was measured by means of ADV's. The available equipment for this purpose was a high-resolution acoustic velocimeter used to measure turbulence and 3D water velocity. A horizontal array of 2 ADVs was set over the breakwaters for both typologies (see Figures 1 and 2), respectively.

The ASTARTE Deliverable D5.21 includes much more details and explanations on the materials that were used to construct the models, the construction process itself, the porosity and sizes of the

stones set in each layer and armor, the exact geometry and location of the structures in the flume, the characteristics and location of the devices that are part of the instrumentation, etc.

4. ON THE GENERATION OF TSUNAMI WAVES IN THE LABORATORY

Solitary waves have been frequently used in laboratory experiments to simulate tsunami waves, (Synolakis, 1987, Borthwick et al., 2006, Esteban et al., 2014, Arikawa et al., 2012, Guler et al. 2015). The hydrodynamics of the phenomena are somehow incomplete using a solitary wave (Madsen et al. 2008) due to the fact that the "tail" of the tsunami is not included in the solitary wave shape, and recent studies have used or developed other approaches, wave shapes and methods, as discussed by Kanoglu et al. (2015). Rossetto et al. (2011) and Goseberg et al. (2013) used a pneumatic and a pump-driven wave maker, respectively. Schimmels et al. (2015) generated more realistic wave shapes using real tsunami records generated with a piston type wavemaker. All these shapes and methodologies have their own pros and cons in their way to simulate tsunamis in the laboratory, but the complete and adequate representation of a whole actual tsunami shape to be used on an appropriate scaled model is still in development. Realistic wave shapes methods represent more accurately the tsunami wave but they are only feasible at small scales, as it is physically unapproachable to include the whole wave at big scales in the present laboratory facilities. But the study of the stability requires a bigger scale in order to avoid scale effects. In this work, the assessment is focused on the calculation of the stability of RMB under tsunami waves, and, consequently, an adequate scale of 1/20 was chosen and the tsunami wave generation method was adopted in accordance. Therefore, in this work, the action of the tsunami on the RMBs was split in 2 parts: the first impact and the overflow.

Armor damage caused by the first solitons impact on RMBs were simulated by means of solitary waves. In addition, the subsequent action of the tsunami overflow, as well as the damage it prompts, was simulated by creating a current using the flume recirculation system and the flume filling pumps.

4.1. Solitary wave tests

Solitary wave heights ranging from 0.20 m to 0.45 m were generated in the laboratory (4 to 9 m in prototype), triggering heavy run-up and overtopping over the tested RMBs (see Figure 6 for type I and Figure 7 for type II RMB).

Figure 6. Solitary wave impacting on type I RMB. The impact generates an overtopping that triggers damage on the leeside of the structure

Tsunamis are commonly studied as a unique wave, contrary to wind waves studies, considering its damage as punctual and explosive, even if, in prototype, more than one soliton-type wave is expected associated to the same tsunami event. To include this aspect, each solitary wave experiment was repeated 5 times, without restoring the geometry, in order to obtain also the accumulated damage due to 2, 3, 4 and 5 consecutive equal waves. This accumulated test introduces the influence of the number of waves in the final damage of the structure.

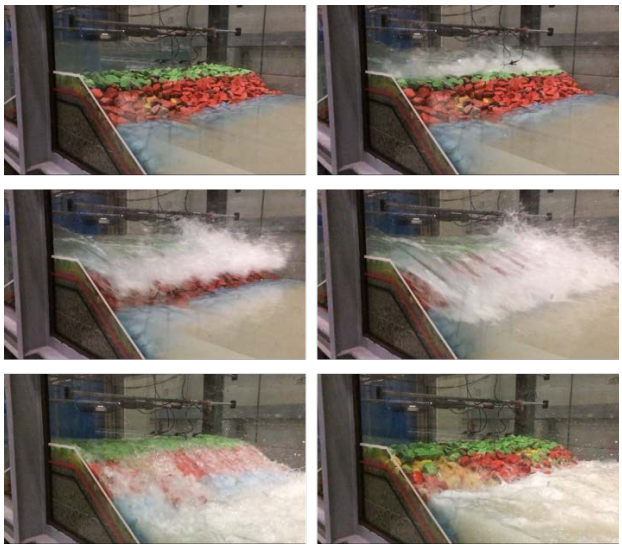

Figure 7. Lateral view of rubble-mound breakwater without crown wall (type II) under solitary wave test

After each wave, the flume was drained to allow the measurement of the damage using photography, visual counting of the displaced stones and by laser profiling. After each wave height set (5 equal waves), the flume was drained and the breakwater was restored to the original condition after the 5th wave of same height. Then, the next set of five solitary wave experiments were conducted increasing

the wave height 5 cm respective to the previous one. Experiments with solitary waves started with 20 cm wave height and concluded in the case of filter layer exposure or when the five experiments with 45 cm wave height were conducted. A summary of the solitary wave experiments that were conducted is given in the Table 1.

Table 1. Solitary wave experiments conducted, given by the wave height and the number of waves, for each typology of RMB.

Wave height in the model (m)	Wave height in the prototype (m)	Number of waves Type I	Number of waves Type II
0.2	4.0	5	5
0.25	5.0	5	5
0.3	6.0	5	5
0.35	7.0	5	5
0.4	8.0	5	3*
0.45	9.0	5	2*

*: For that wave height and number of waves, destruction was reached

4.2. Overflow tests

The overflow tests were carried out after the solitary wave tests for each RMB type, using the flume recirculation and filling systems. Overflow experiments consisted of the recirculation of water to create a steady current that generates a difference in the water level at both sides of the structure, triggering an overflow over the top of both typologies of breakwaters (see type II in Figure 8). The overflow height, Ho, is defined here as the vertical distance between the breakwater crest and the seaside water level before the backwater curve.

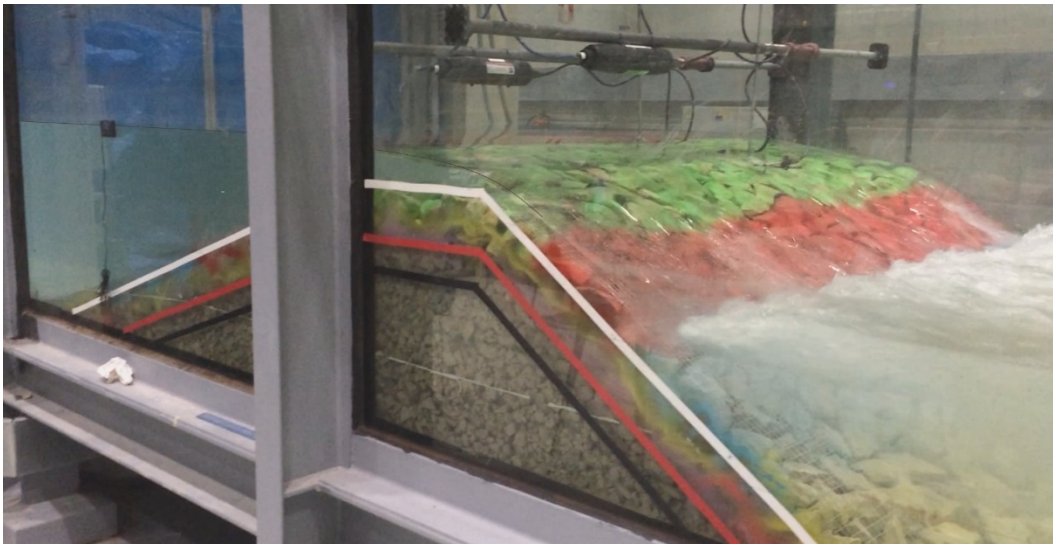

Figure 8. Lateral view of rubble-mound breakwater without crown wall (type II) under overflow current.

The pumps started the recirculation, increasing the seaside water level until the breakwater crest level was achieved. At this stage, the pumps reproduce a typical overflow curve, assuming a pseudo-triangular increase and decrease of the overflow height (see Figure 9). The tests were determined by two parameters: (1) the time period, T_o, and (2) the overflow height, Ho. The maximum value of the overflow height reached during the experiment is the "peak overflow height", H_p, The experiments were carried out increasing H_p, from 3.5 cm (70cm in prototype), until armor destruction. For each overflow, T_o values of 1, 2, 3, 4 and 5 minutes were used. To reach the highest overflow heights, the flume filling pumps were also used, adding water to the system.

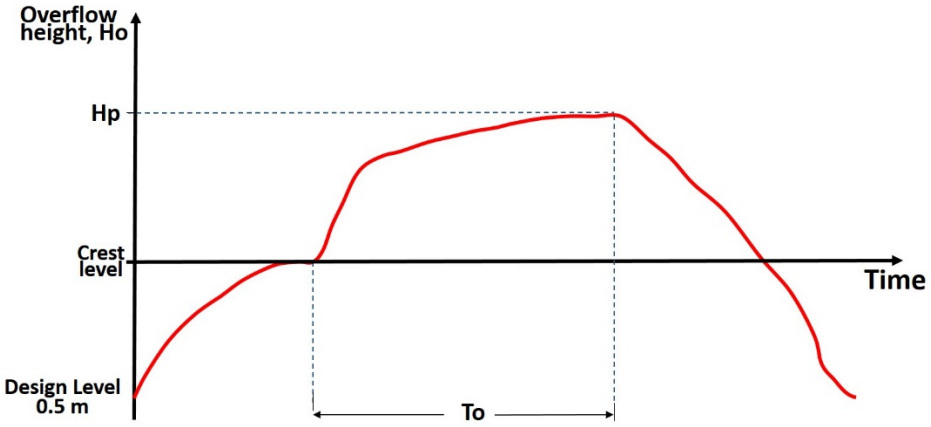

Figure 9. Scheme of evolution of the overflow height, Ho, during overflow experiments. Hp is the peak height obtained and To is the time to achieve Hp from the crest level using the flume recirculation and filling system.

Like in the case of solitary wave experiments, after each test the flume was drained to allow the damage measurement. Then the breakwater was restored to the original conditions before the next experiment.

5. STABILITY ASSESSMENT VARIABLES

There are several variables to be calculated in the analyses of RMB stability based on laboratory experiments. In general terms, among those variables can be mentioned the armor units nominal diameter, the armor units weight distribution, armor units density, their relative submerged density, the significant wave height Hs, the averaged wave period, Tm, the armor slope angle, α, the average eroded area Ae and the number of waves N.

In this case, the laboratory experiments characteristics allow analyzing the influence of some of them that can be grouped in three main non-dimensional parameters: The stability number, Ns, the damage parameter, S, and the number of waves, N.

The stability number Ns (Hudson, 1959), is frequently used, defined as:

$$Ns=H/(\Delta^* D_{n50}) \quad (1)$$

In the following, the solitary wave height, H, will be used to define the stability number in the solitary wave tests, as proposed by Esteban eta al. (2014), while peak overflow height, Hp, will be used to define this parameter in the overflow tests. The stability numbers realized in the laboratory experiments with solitary waves are those given in Table 2.

Table 2. Stability number values for seaside and leeside armors and for both RMB typologies

H	Type I seaside and Type II seaside and leeside (D_{n50}=74.7 mm)	Type I Leeside (D_{n50}=34.1 mm)
0.20	1.62	3.55
0.25	2.02	4.44
0.30	2.43	5.33
0.35	2.83	6.22
0.40	3.24	7.11
0.45	3.65	8.00
0.50	4.06	8.89

The damage parameter calculation on a RMB can be achieved following several methodologies (Vidal et al., 2003 [33]), and it is commonly tackled by calculating the so-called damage parameter (Broderick, 1984 [34]), defined as:

$S=Ae/ D_{n50}^2$ (2)

Where Ae is the mean eroded area in the structure section.

For prototypes, the eroded area is calculated by comparing the geometry before and after the damage. In the laboratory, this geometry change was measured both with a laser profiler, and counting displaced stones, using the expression:

$Ae= (Ne*D_{n50}^3) / ((1-n)*L)$ (3)

where Ne is the number of extracted stones, n is the armor layer bulk porosity and L the width of the studied section. In these experiments, to avoid the side flume glass walls influence on the armor damage, only a 1.7 m-wide central portion of the flume was used to assess the damage, leaving 15 cm strips near the walls without damage assessment (see Figure 10).

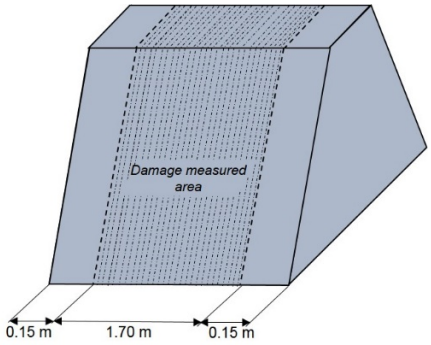

Figure 10. Type II RMB area where damaged was measured counting displaced stones.

The armor damage due to wind waves is commonly classified following a qualitative criteria.

(1) Initiation of Damage (Id), when the upper armor layer has lost some units, and the space among stones is clearly wider than the design porosity;

(2) Initiation of Iribarren's Damage (IId), when damage in the upper armor layer expose completely the bottom armor layer to the wave flow action and its units could be extracted.;

(3) Initiation of Destruction (ID), defined as the initiation of damage of the lower armor layer, when some units from this layer has been removed; and

(4) Destruction (D), when several units have been removed from the filter layer.

Vidal et al 1994 [38], set for wind waves the damage parameter threshold values for each criteria, depending on the armor slope angle (see Table 3).

Table 3. Threshold values for damage parameter, S, and armor slope, α, for the tested RMBs.

		Threshold values for damage parameter, S			
	Cot α	Id	IId	ID	D
Leeside slope	1.5	1.0	2.5	6.5	12
Seaside slope	3.0	2.5	3.5	9.5	16

6. RESULTS

The stability number and the damage parameter have been calculated for each RMB typology (type I with crown wall, type II without crown-wall), and at both sides of the structures separately (seaside, including crown, and leeside). Following, the results at each type and side are detailed.

6.1. Results of the solitary wave experiments (SW)

The stability number and the damage parameter have been calculated for each RMB typology (type I with crown wall, type II without crown-wall), and at both sides of the structures separately (seaside slope, including crown, and leeside slope). Following, the results for each type and side are detailed.

6.1.1. Analysis of the damage on the Seaside of Type I RMB

For the type I RMB, no damage was visible in the seaside until the solitary wave height reached 25 cm (5 meters in the prototype). In this case several units' extractions in the outer armor were observed. As the wave height increased a very slow increase on the damage was observed. The solitary wave tests finished with the 45 cm wave height series (9 m in prototype) and the damage only affected the first layer of the armor. All the extracted stones in this side of the structure were dragged down the seaside armor.

The values of the damage parameter of the seaside for each experiment on type I RMB are given in the Table 4.

Table 4. Type I. Seaside damage parameter, S, results. Cell without value indicates that damage was not measured

		Number of Waves, N				
		1	**2**	**3**	**4**	**5**
Solitary	**0.2**	0	0	0	0	0
	0.25	0.04	0.04	0.04	0.17	0.26

	0.3	0.09	0.17	0.35	0.44	-
	0.35	0.17	0.48	0.65	0.96	1.09
	0.4	0.57	1.09	1.39	1.52	2.26
	0.45	0.65	1.22	1.65	2.31	2.53

In general, the reached damage was low, and just for the maximum height the Initiation of Damage is reached.

6.1.2. Analysis of the damage on the Seaside of Type II RMB

A similar analysis like that conducted for the type I RMB can be followed for the type II RMB, in its seaside. In this case, the damage is, in general terms, lower than in the type I seaside. This is due to the fact that the crown-wall action prompts the reflection and run-down of the wave, dragging the units down the armor.

The values of the damage parameter on the seaside for each experiment on type II RMB are given in the Table 5.

Table 5. Type II. Seaside damage parameter, S, results. Cell without value indicates that damage was not measured because the leeside slope destruction was reached in previous experiment.

		Number of Waves, N				
		1	**2**	**3**	**4**	**5**
Solitary Wave Height H	**0.20**	0	0	0	0	0.09
	0.25	0.04	0.3	0.52	0.57	0.7
	0.30	0.09	0.3	0.39	0.44	0.57
	0.35	0.35	0.44	0.83	0.87	0.96
	0.40	0.65	1.13	1.35	-	-
	0.45	0.96	1.65	-	-	-

6.1.3. Type I and type II seaside joined analysis

In the seaside slope, solitary waves surge on the slope, overtopping the breakwater. During the run-up flow, armor stones can be displaced forward from the front slope and the crest. Besides the wave influence, the outer slope upwards displacement of armor stones should increase for decreasing slope angles. After the wave passage, the run-down flow could also trigger armor displacements that should increase with increasing crest freeboard (less overtopping implies more run-down flow) and with increasing slope angle. For the seaside slope armor, the small damage differences found between Type I and II structures can be blamed to the crown wall effect that produces a small increment in the down rush flow.

6.1.4. Analysis of the damage on the Leeside of Type I RMB

As indicated above, the plywood crown wall, was fixed to the RMB core. When impacted by the solitary wave run-up, the overtopping flow fell on the horizontal plate, which deflected the flow to the lee side. This deflected jet impacted on the water, that acted as a stilling basin, reducing the action on the submerged backslope armor, that in consequence suffered only minor damage, see Figure 11.

Regarding the backslope damage, it is very stable when the overtopping flow impinges on the lee side water. For RMBs without crown wall this situation occurs when the breakwater freeboard is very low or negative. In type I breakwater, the crown wall horizontal plate, located near the free surface, always deflects the flow away from the backslope, so minor damage is produced. Other crown wall configurations, with higher horizontal plates could produce jets impacting on the backslope with presumably higher damages. Another particular behavior of the backslope armor stability is that this section is very fragile, meaning that the damage progression is very fast, both with the number of waves or with increasing wave height.

Figure 11. View of rubble-mound breakwater with crown wall (type I) under solitary wave test.

In this particular laboratory experiments, the size of the leeside slope armor units, Dn50, is smaller than in the seaside slope. That means that for the same wave height, the Ns value of the backslope armor is higher (see equation 1). Even with these higher values of Ns, the damage parameter maximum value has been S = 0.71 (see Table 6), result that do not allow a fit between S, N and Ns.

Table 6. Type I. Solitary wave tests. Leeside slope damage parameter, S, results.

		Number of Waves, N				
		1	2	3	4	5
Solitary Wave Height H	0.2	0	0	0	0	0
	0.25	0	0	0.12	0.12	0.12
	0.3	0	0.04	0.1	0.12	0.18
	0.35	0.04	0.04	0.12	0.14	0.14
	0.4	0	0.24	0.38	0.52	0.71
	0.45	0.02	0.12	0.16	0.34	0.5

6.1.5. Analysis of the damage on the Leeside of Type II RMB

For the case of the type II RMB leeside, the overtopping flow impinges on the back slope, (see Table 7) and the damage is noticeable from the tests with 20 cm wave height (4 meters in prototype)and for 0.3 m wave height, the initiation of damage is reached after the 5th wave of the set. For 0.35 m wave height, the initiation of damage appears after the 3rd wave and the initiation of Iribarren damage is clearly reached after the 4th wave of the set. Finally, for the 0.4 m wave (8m in prototype) the initiation of destruction is reached in the 2nd wave and the destruction is patent after the 4th wave. This fast evolution of damage is in agreement with the above indicated fragility of the backslope armor stability.

The values of the damage parameter that were calculated for the leeside of the type II RMB are given in Table 7.

Table 7. Type II. SW tests. Leeside damage parameter, S, results.

		Number of Waves, N				
		1	2	3	4	5
Solitary Wave Height H	0.2	0	0	0	0	0
	0.25	0.44	0.7	0.87	1.13	1.35
	0.3	0.52	0.78	1.04	1.74	2.92
	0.35	0.39	1.61	2.09	5.09	7.71
	0.4	7.05	12.45	20	-*	-*
	0.45	2.31	9.58	-*	-*	-*

*: For that wave height, leeside slope destruction was reached in previous experiment

6.2. Results of the overflow currents experiments

For the case of steady currents over the structures, the damage was measured following the same methodology as in the solitary wave experiments. However, in this case, the current was not able to extract stones easily and therefore, the damage was null or minimum in most of the tests. Following, the behavior of both RMB, type I and II, under the overflow is described.

6.2.1. Analysis of the behavior of the type I RMB under overflow

For type I RMB the maximum peak overflow height, achieved using the flume recirculation pumps was Hp=6.7 cm over the crown wall level (1.34 m in the prototype), and damage was not observed, neither in seaside nor in leeside. To increase the overflow, flume filling pumps were used to add water in the seaside to the recirculation flow. As a result, the peak height reached a value of Hp=15.1 cm over the crown wall (3 m in the prototype). The damage in the seaside was null, as the direction of the current does not tend to displace the armor units and just a few extractions were observed in the leesideasthe protective action of the crown-wall avoided more extractions (Figure 12). The action on the submerged part of the leeside armor was minimum.

Figure 12 . Overflow current. Type I RMB. The overtopping flow falls on the horizontal plate.

The experiment finished when, due to the added water, the level at both sides of the structure was equal and no damaged was observed.

6.2.2. Analysis of the behavior of the type II RMB under overflow

In the overflow tests on type II RMB, the flume recirculation system allowed to reach a peak overflow height of Hp=7 cm (1.4 m in the prototype). No extraction of armor units was observed.

Following the same procedure as in the type I RMB, the flume filling pumps were added and, as a consequence, some extractions appeared in the back slope for a peak overflow height of Hp=11 cm (2.2 m in prototype). The overflow was gradually increased but the damage remained very low. Finally, RMB backslope collapsed for a peak overflow height of Hp=11.7 cm (2.34 m in prototype) after 1 minute of overtopping (see Figure 13).

Figure 13. Top view of the type II model damage after overflow tests

No damage was noticed in the seaside and previous damage in leeside was negligible. In order to strengthen this result, the whole series of experiments was repeated and the structure destruction was reached in the very same instant, after 2 minutes of 11.7 cm free surface elevation over the structure.

In the Table 8, the damage parameter obtained for overflow experiments on RMBs leeside is summarized. The damage on seaside slopes of both typologies was negligible, and they are not included in Table 8.

Table 8. Overflow tests. Leeside damage parameter, S, results.

		TYPE II		TYPEII		TYPE I	
		Series I		Series II		Series I	
	To (minutes)	**Hp(cm)**	**S**	**Hp(cm)**	**S**	**Hp(cm)**	**S**
Recirculation Pumps	1	3.5	0	3.5	0	3.5	0
	2	3.5	0	3.5	0	3.5	0
	3	3.5	0	3.5	0	3.5	0
	4	3.5	0	3.5	0	3.5	0
	5	3.5	0	3.5	0	3.5	0
	1	4.7	0	4.7	0	4.7	0
	2	4.8	0	4.8	0	4.8	0
	3	4.9	0	4.9	0	4.9	0
	4	4.9	0	4.9	0	4.9	0
	5	4.9	0	4.9	0	4.9	0
	1	6	0	6	0	6	0
	2	6.6	0	6.6	0	6.6	0
	3	6.7	0	6.7	0	6.7	0
	4	6.7	0	6.7	0	6.7	0
	5	6.7	0	6.7	0	6.7	0
Recirculation + filling pumps	1	7.9	0	7.2	0	7.2	0
	2	8.3	0.087	7.5	0.087	7.2	0
	3	8.3	0	8.2	0	7.5	0
	4	8.5	0	7.5	0	7.5	0
	5	8.7	0	7.8	0	7.5	0
	1	10	0	10.3	0	10.2	0
	2	11.2	1.3	11.3	1.3	11.2	0
	3	12	0.348	12	0.348	12	0
	4	12.6	0.609	12.7	0.609	12.4	0
	5	12.6	0.609	12.7	0.609	12.4	0
	1	11.7	Destruction	11.7	0.609	11.3	0
	2	-	-	11.7	Destruction	12.3	0
	3	-	-	-	-	14.6	0.039
	4	-	-	-	-	15.1	0.23

Tsunami-like solitary waves can prompt greater damage that wind waves but following the same pattern. But steady current damage is explosive, and normally, if the Initiation of Iribarren´s damage is reached during one test, the structure reaches destruction very quickly.

7. CONCLUSIONS

7.1. Regarding solitary waves tests

Stability of front slope armor stones: In the seaside slope, solitary waves surge on the slope, overtopping the breakwater. During the run-up flow, armor stones can be displaced upwards from the front slope and the crest. Besides the wave height, the outer slope upwards displacement of armor stones should increase for decreasing slope angles. After the wave passage, the run-down flow could also trigger armor displacements that should increase with increasing crest freeboard (less overtopping implies more run-down flow) and with increasing slope angle. For the seaside slope armor, the small damage differences found between Type I and II structures can be blamed to the crown wall effect that produces a small increment in the down rush flow.

Stability of back slope armor stones: The back slope stability depend, besides wave height and number of waves, on the overtopping flow discharge (which in turn depend on crest freeboard) and the back slope area that is directly affected by this discharge. This area prone to be damaged is different in structure Type I and II. As the crown-wall was fixed to the core, the failure mechanism related to sliding of crown-wall was not considered. On the other hand, the fixed crown-wall allowed a more accurate measurement of the hydrodynamics in the process. Files containing the measurement of pressures, heights and velocities were included in the D4.20, what will lead to further analyses of the crown wall, basically regarding pressures and loadings.

Type I back slope stability: In the case of structure Type I, the overtopping flow falls on the road behind the crown wall and due to the low elevation of the road over the sea level, the resulting water flow is jetted to the water behind the breakwater that acts as stilling basin causing minimum action over the back slope armor. For a given crest freeboard, for this typology higher road levels should increase the damage. Back slope angle effect is contradictory: higher slope angles will decrease the area prone to damage (decreasing de damage) but also decrease the stability of the armor units (increasing the damage).

Type II back slope stability: In the case of Type II breakwater, the overtopping flow run-down over back slope, dragging downward the armor units. Again, low crest levels will increase overtopping discharges but decrease the back slope area prone to damage and the downward velocities. On the contrary, high crest levels will decrease the overtopping flow, but increase downward velocities. From the previous reasoning, the freeboard causing maximum back slope damage should be somewhere between the freeboard of no overtopping and the cero freeboard, when there is no direct wave action on the back slope armor units. This back slope stability behavior was demonstrated by Vidal et al. (1992). Back slope angle effect is also contradictory: higher slope angles will decrease the area prone to damage (decreasing the damage) but also decrease the stability of the armor units (increasing the damage).

Figure 14 . Destruction of the type II RMB after the 3rd wave of 0.4 m.

7.2. Regarding steady current tests

Complementing solitary wave laboratory experiments, overflow current experiments were conducted. These tests were carried out varying the overflow height Hp, from 3.5 cm (70 cm in the prototype) to 15 cm (3m in prototype) for type I RMB, and to 12.7 cm (2.54 m in prototype) for type II RMB.

In the seaside, the current going through the structure is not a demanding load for the armor units for both types of RMB. The flow, itself, pushes the units towards the structure, and therefore, no extractions are noticed and the damage is null.

On the other hand, the flow affects the leeside of the structures in 2 ways. Firstly, as the flow is going through the structure layers from seaside to leeside, a force in the direction of the flow is acting and boosting the extraction of units from the inside. In addition, the difference of level between both sides of the RMBs, triggers an overflow that falls directly into the structure, dragging downwards the armor units.

In the case of the type I RMB, that overflow falls on the road behind the crown, reducing the energy that reaches the units of the leeside. The gravity influence is bigger than the action of the current through the structure plus the overflow impact, and thus, no extraction is then noticed for this layer, and the damage can be considered as negligible. In this case, the structure presents an adequate behavior. In the Table 8, it was observed how the damage due to the lower overflow heights is null. Obviously, other geometries would lead to new scenarios that complement these results, for instance by using other crown-wall widths and relating this value with the Hp and the triggered damage S. In this sense, Takagi et al (2014) already highlighted the influence of the crown-wall width in the final damage on the coastal structures due to the 2011 tsunami in Japan.

In the case of the type II RMB, high crest levels increase downwards velocities acting directly on the units of the leeside armor. In this sector, destruction occurred suddenly when the peak overflow height reached Hp=12 cm. Once a few units are extracted, the damage growth is unstoppable, and the structure collapses quickly, reaching its destruction.

The overflow experiments on type II RMB were conducted twice, and the destruction was reached for both series when Hp=12 cm (27 cm over the design water level). This result allows to affirm that the collapse was reached for a Stability Number Ns=2.18 (eq. 1), following the equation 1.

This laboratory experiments as well as a further analysis of the results are included in the paper "Stability of rubble-mound breakwaters under tsunami first impact and overflow based on laboratory experiments", under review in Coastal Engineering Elsevier Journal.

REFERENCES

Í. Aniel-Quiroga, C. Vidal, J.L. Lara, M. González, F.F. Jaime, Á. Álvarez, LABORATORY EXPERIMENTS ON RUBBLE-MOUND BREAKWATERS UNDER TSUNAMI WAVE, in: Proc. 6th Int. Conf. Appl. Phys. Model. Coast. Port Eng. Sci., 2016.

T. Arikawa, M. Sato, K. Shimosako, I. Hasegawa, G.-S. Yeom, T. Tomita, Failure Mechanism of Kamaishi Breakwaters due to the Great East Japan Earthquake Tsunami, in: Coast. Eng. Proc., 2012: p. 13. doi:10.9753/icce.v33.structures.16.

R. Asakura, K. Iwase, T. Ikeya, M. Takao, T. Kaneto, N. Fujii, U. M, The tsunami wave force acting on land structures, in: Proc. 28th Int. Conf. Coast. Eng. ASCE, 2002: pp. 1191–1202.

A.G.L. Borthwick, M. Ford, B.P. Weston, P.H. Taylor, P.K. Stansby, Solitary wave transformation, breaking and run-up at a beach, Proc. Inst. Civ. Eng. - Marit. Eng. 159 (2006) 97–105. doi:10.1680/maen.2006.159.3.97.

L. Broderick, Riprap stability versus monochromatic and irregular waves, 1984. doi:10.1300/J082v36n01.

M. Esteban, M. Izumi, S. Tomoya, R. Aranguiz, T. Mikami, N.D. Thao, K. Ohira, A. Ohtani, STABILITY OF RUBBLE MOUND BREAKWATERS AGAINST SOLITARY WAVES, in: ICCE 1012, International conference on coastal engineering (ICCE) 2012, 2012: pp. 1–13.

M. Esteban, R. Jayaratne, T. Mikami, I. Morikubo, T. Shibayama, N.D. Thao, K. Ohira, A. Ohtani, Y. Mizuno, M. Kinoshita, S. Matsuba, Stability of Breakwater Armor Units against Tsunami Attacks, J. Waterw. Port, Coastal, Ocean Eng. 140 (2014) 188–198. doi:10.1061/(asce)ww.1943-5460.0000227.

A. Etemad-Shahidi, M. Bali, Stability of rubble-mound breakwater using H50 wave height parameter, Coast. Eng. 59 (2012) 38–45. doi:10.1016/j.coastaleng.2011.07.002.

M.E. Gómez-Martín, J.R. Medina, Heterogeneous Packing and Hydraulic Stability of Cube and Cubipod Armor Units., J. Waterw. Port, Coast. Ocean Eng. 140 (2014) 100–108. doi:10.1061/(ASCE)WW.1943-5460.0000223.

N. Goseberg, A. Wurpts, T. Schlurmann, Laboratory-scale generation of tsunami and long waves, Coast. Eng. 79 (2013) 57–74. doi:10.1016/j.coastaleng.2013.04.006.

H.G. Guler, T. Arikawa, T. Oei, A.C. Yalciner, Performance of rubble mound breakwaters under tsunami attack, a case study: Haydarpasa Port, Istanbul, Turkey, Coast. Eng. 104 (2015) 43–53. doi:10.1016/j.coastaleng.2015.07.007.

M. Hanzawa, A. Matsumoto, H. Tanaka, STABILITY OF WAVE-DISSIPATING CONCRETE BLOCKS OF DETACHED breakwaters against tsunami, ICCE 2012 Proceeding. (2012) 2–7.

R.Y. Hudson, Laboratory investigation of rubble mound breakwaters, J. Waterw. Port, Coast. Ocean Div. ASCE. 85(3) (1959) 93–121.

R.Y. Hudson, F.A. Herrmann, R.A. Sager, R.W. Whalin, G.H. Keulegan, C.E. Chatham, L.Z. Hales, Coastal Hydraulic Models, special report No. 5, 1979.

S.A. Hughes, Physical Models and Laboratory Techniques in Coastal Engineering, 1993.

R. Iribarren, Una fórmula para el cálculo de los diques de ecollera, (1938).

R. Iribarren, Fórmula para el cálculo de los diques de escolleras naturales o artificiales, (1965).

U. Kanoglu, V.V. Titov, E.N. Bernard, C.E. Synolakis, Tsunamis: bridging science, engineering and society, Philos. Trans. R. Soc. 373 (2015) 1–24. doi:10.1098/rsta.2014.0369.

F. Kato, S. Inagaki, M. Fukuhama, Wave force on coastal dike due to tsunami, Coast. Eng. (2006) 5150–5161. http://pwweb1.pwri.go.jp/eng/ujnr/joint/37/paper/13kato.pdf.

F. Kato, Y. Suwa, K. Watanabe, S. Hatogai, Mechanisms of Coastal Dike Failure Induced By the Great East Japan Earthquake Tsunami, Coast. Eng. Proc. 1 (2012). doi:10.9753/icce.v33.structures.40.

M.A. Losada, J.M. Desire, L.M. Alejo, Stability of Blocks as Breakwater Armor Units, J. Struct. Eng. 112 (1986) 2392–2401. doi:10.1061/(ASCE)0733-9445(1986)112:11(2392).

M.A. Losada, L.A. Gimenez-Curto, The joint effect of the wave height and period on the stability of rubble mound breakwaters using Iribarren's number, Coast. Eng. 3 (1979) 77–96. doi:10.1016/0378-3839(79)90011-5.

P.A. Madsen, D.R. Fuhrman, H.A. Schaffer, On the solitary wave paradigm for tsunamis, J. Geophys. Res. 113 (2008). doi:10.1029/2008JC004932.

O.T. Magoon, R.L. Sloan, G.L. Foote, DAMAGES TO COASTAL STRUCTURES, Coast. Eng. Proc. 1 (1974).

J.R. Medina, Y. Vidal, Diseño y construcción de diques rompeolas Design and construction of mound breakwaters, (2014). doi:10.4995/ia.2014.3074.

T. MIKAMI, T. SHIBAYAMA, M. ESTEBAN, R.Y.O. MATSUMARU, FIELD SURVEY OF THE 2011 TOHOKU EARTHQUAKE AND TSUNAMI IN MIYAGI AND FUKUSHIMA PREFECTURES, Coast. Eng. J. 54 (2012) 1250011. doi:10.1142/S0578563412500118.

S. Mizutani, F. Imamura, Dynamic wave force of tsunamis acting on a structure, ITS 2001 Proc. (2001) 941–948.

N. MORI, T. TAKAHASHI, Nationwide Post Event Survey and Analysis of the 2011 Tohoku Earthquake Tsunami, Coast. Eng. J. 54 (2012) 1250001. doi:10.1142/S0578563412500015.

W.H. Munk, The Solitary Wave Theory And Its Application To Surf Problems, Ann. N. Y. Acad. Sci. 51 (1949) 376–424. doi:10.1111/j.1749-6632.1949.tb27281.x.

I. Nistor, D. Palermo, Y. Nouri, T. Murty, M. Saatcioglu, Tsunami-Induced Forces on Structures, Handb. Coast. Ocean Eng. (2009) 261–286. doi:doi:10.1142/9789812819307_0011.

E.A. Okal, H.M. Fritz, P.E. Raad, C. Synolakis, Y. Al-Shijbi, M. Al-Saifi, Oman Field Survey after the December 2004 Indian Ocean Tsunami, Earthq. Spectra. 22 (2006) 203–218. doi:10.1193/1.2202647.

T. Rossetto, W. Allsop, I. Charvet, D.I. Robinson, Physical modelling of tsunami using a new pneumatic wave generator, Coast. Eng. 58 (2011) 517–527. doi:http://dx.doi.org/10.1016/j.coastaleng.2011.01.012.

S. Schimmels, V. Sriram, I. Didenkulova, Tsunami generation in a large scale experimental facility, Coast. Eng. 110 (2015) 32–41. doi:10.1016/j.coastaleng.2015.12.005.

C.E. Synolakis, L. Kong, Runup measurements of the December 2004 Indian Ocean tsunami, Earthq. Spectra. 22 (2006). doi:10.1193/1.2218371.

C.E. Synolakis, The runup of solitary waves, J. Fluid Mech. 185 (1987) 523. doi:10.1017/S002211208700329X.

H. Takagi, J.D. Bricker, ASSESSMENT OF THE EFFECTIVENESS OF GENERAL BREAKWATERS IN REDUCING TSUNAMI INUNDATION IN ISHINOMAKI On 11 March , 2011 , a large earthquake that occurred off the north – east coast of Japan generated a large tsunami which devastated extensive areas of the, 56 (2014) 1–21. doi:10.1142/S0578563414500181.

S. Thorndike, WAVE RUN-UP ON COMPOSITE SLOPES, (1949).

T. TOMITA, G.-S. YEOM, M. AYUGAI, T. NIWA, Breakwater Effects on Tsunami Inundation Reduction in the 2011 off the Pacific Coast of Tohoku Earthquake, J. Japan Soc. Civ. Eng. Ser. B 2(Coastal Eng. 68 (2012) 4–8.

J. van der Meer, Stability of Rubble Mound Slopes under Random Wave Attack, in: ICCE 1984 Proceeding, 1984: pp. 2620–2634.

J. Van der Meer, Stability of breakwaters Armour Layers - Design Formulae, (1987).

C. Vidal, M.A. Losada, R. Medina, E.P.D. Mansard, G. Gomez-Pina, A UNIVERSAL ANALYSIS FOR THE STABILITY OF BOTH LOWCRESTED AND SUBMERGED BREAKWATERS, Coast. Eng. Proc. 1 (1992).

C. Vidal, R. Medina, P. Lomónaco, Wave height parameter for damage description of rubble-mound breakwaters, Coast. Eng. 53 (2006) 711–722. doi:10.1016/j.coastaleng.2006.02.007.

C. Vidal, I.J. Losada, F.L. Martin, STABILITY OF NEAR-BED RUBBLE-MOUND STRUCTURES, Coast. Eng. Proc. 1 (1998).

C. Vidal, M.A. Losada, R. Medina, STABILITY OF MOUND BREAKWATER'S HEAD AND TRUNK, (1991).

C. Vidal, M.A. Losada, R. Medina, E.I. Losada, Analisis de la estabilidad de diques rompeolas, 1 (1994) 17–34.

C. Vidal, F.L. Martin, V. Negro, X. Gironella, B. Madrigal, J. García-Palacios, Measurement of Armor Damage on Rubble Mound Structures: Comparison Between Different Methodologies, in: Coast. Struct. 2003, American Society of Civil Engineers, Reston, VA, 2004: pp. 189–200. doi:10.1061/40733(147)16.